6

Gas Mixing in the Lung Periphery

MANUEL PAIVA

Institute of Interdisciplinary Research
Free University of Brussels
Brussels, Belgium

LUDWIG A. ENGEL

Westmead Hospital
Sydney, New South Wales, Australia

In humans, more than 95% of the lung volume is peripheral to the respiratory bronchioles, that is, more than 19 out of 20 molecules of gas in the lung are within the acini. Because of the small dimensions of the respiratory bronchioles and alveolar ducts and the intricate way these branches are interconnected, gas concentrations cannot be measured directly. The isotopic techniques, from which most of the in situ concentration measurements are computed, allow only the study of pools of hundreds of acini. Therefore, our knowledge of the mechanisms of transport and mixing in the lung periphery derives mainly from modeling studies and indirect experimental observations.

In the past, we have favored the elaboration of models of a system, that is, models based upon anatomical data and laws of physics. The model simulates experiments and from the differences between simulations and

This work was supported partly by a contract with the Ministère de la Politique Scientifique (Actions Concertées), by contract 3.4521.87 between the Fonds de la Recherche Scientifique Médicale of Belgium and the Free University of Brussels, and by National Institutes of Health Grant HL 26330.

experiments one can critically reexamine the assumptions upon which the model is based. Because no parameter fitting is performed, the inability of the model to reproduce experimental data may give some insight into underlying mechanisms. A model of a system is only of value if it can answer questions of physiological interest. A model may be intrinsically beautiful from the mathematical point of view or from the generality of the physical laws used and yet totally useless for physiologists. Because simulating the entire respiratory system faithfully is an impossible task in the foreseeable future, a model should be built in relation to questions asked. From all models satisfactorily answering a physiological question, the simplest one is the best. Once a model is elaborated, it should be used to suggest new experiments that may validate or disprove it. It can also be used to test different hypotheses.

The development of a model of a system requires a continuous feedback between experimental results and model assumptions. A model of a system is always perfectible. The constant interaction between experiments and simulations will be the underlying philosophy of this chapter. Extensive reviews have been recently published on both the experimental and theoretical studies of gas mixing and ventilation distribution in the lung (Engel, 1983, 1985, 1986; Paiva, 1985; Paiva and Engel, 1987; Piiper and Scheid, 1987). Therefore, we restrict this chapter to those aspects of the topic in which the experimental-theoretical interaction has been particularly fruitful.

The modeling of gas mixing in the periphery of the lung benefited from some favorable circumstances that resulted in a rapid development of this area of research: in the early 1960s, Weibel (1963) gave a detailed quantitative description of the lung. This coincided with the development of fast digital computers, making possible the numerical integration of mathematical equations derived from classical physics.

I. Diffusion Front

A. Experimental

Measurements In Lungs

In 1973 Engel et al. (1973a) described a new method of sampling from intrapulmonary airways using a retrograde catheter 1.5 mm in external diameter. When N_2 concentration was sampled in airways with a diameter as small as 2.5 mm, during inspiration of O_2 at a constant flow, the N_2 concentration did not reach zero (Engel et al., 1973b). Furthermore, although the N_2 concentration oscillated synchronously with heart pulsations, the mean concentration remained almost stationary during the inspiration.

This was the first direct measurement of the diffusion front that separates inspired and resident gas.

Subsequently, Fukuchi et al. (1976) compared intrabronchial N_2 concentration during inspirations of O_2 at a constant flow in vivo and postmortem. They concluded that the mixing action of the heart resulted in an effective diffusion coefficient more than five times greater than that for molecular diffusion. The authors also showed that the diffusion front moves peripherally when increasing the flow or decreasing the lung volume (Fukuchi et al., 1976). Although the N_2 concentration profiles within the lung during an inspiration of O_2 must vary between zero and close to 80% in the alveolar zone, the measured N_2 concentration was always smaller than 10% because only the proximal part of the front could be measured. Therefore, the conclusions on the effective diffusivity due to cardiogenic mixing apply only to the proximal part of the diffusion front and cannot be directly extrapolated to the more peripheral zones of the lung. Horsfield et al. (1982) suggested that the heart action has only a small effect on gas mixing distal to the diffusion front during respiration without breathholding. Jones et al. (1982), using wash in of inert gases, failed to show any effect of the heartbeat on gas mixing, but the method used was probably not sensitive to small variations of mixing efficiency.

Measurements In Lung Casts

The proximal part of the diffusion front was also measured in a hollow cast of the airways of a pig lung (Horsfield et al., 1980). A constant flow of 6.7 ml/sec of N_2 was blown down at the cast entry and O_2 concentrations measured at various points through small holes in the cast. The more peripheral airways had an internal diameter of approximately 0.14 cm and there were about 200 such branches. As the authors explicitly stated, a major difference between gas transport in the cast and in a real lung was related to the determinants of flow. In the open-ended cast, the flow is determined by the resistance of each pathway, whereas in the lung this is achieved mainly by the compliance of the alveolar region.

From the data of Horsfield et al. (1980) it is possible to compute the mean convective velocity at the periphery of the cast as 2.14 cm/sec. This corresponds to a Péclet number greater than one, indicating a transport dominated by convective flow. As in the in vivo experiments already described, only the proximal part of the diffusion front could be measured. Furthermore, this diffusion front is really stationary as the gas concentrations are constant at both ends, whereas in vivo the O_2 concentration in the alveolar sacs increases slightly during inspiration.

B. Theoretical

The introduction of the concept of the diffusion front in the airways of the lung preceded the availability of experimental data. Based on the Weibel model of the lung, Wilson and Lin (1970) proposed that for an O_2 inspiration at a constant flow of 300 ml/sec, a stationary concentration profile (dashed line of Fig.1) was established within the lung. They also proposed a physical mechanism, the front representing an equilibrium between convection tending to sweep N_2 into the terminal airspaces to the left and diffusion tending to empty airspaces of N_2 by diffusion to the right. This work was probably unknown to the three groups who, independently, and using different approaches, suggested the existence of a quasistationary concentration profile during inspiration at a constant flow (Cumming et al., 1971; Paiva, 1972; Scherer et al., 1972).

A major advance in the understanding of the physical mechanisms leading to the diffusion front came from the establishment of a transport equation that describes the (simultaneous) transport by convection and diffusion in the symmetrical lung model of Weibel. When gas transport across the alveolar capillary membrane is neglected, such an equation (Paiva, 1972; Scherer et al., 1972) can be written as

$$\frac{\partial F}{\partial t} = D\frac{s}{S}\frac{\partial^2 F}{\partial x^2} + \frac{D}{S}\frac{\partial s}{\partial x}\frac{\partial F}{\partial x} - u\frac{\partial F}{\partial x}, \qquad (1)$$

where the fractional gas concentration F is a function of time (t) and distance (x) to a fixed point of the model, usually the entry or the alveolar end. s(x) and S(x) are the cross-sectional area of the conducting airways alone, and the total cross-section of airways plus alveoli, respectively. D is the binary diffusion coefficient between inspired and residual gas, and u the convective velocity.

The left side of equation (1), together with the first term on the right, constitute the Fick equation governing unidimensional diffusion under static conditions. The second term on the right takes into account the changing cross-sectional area whereas the third term introduces the convective component of gas transport. The quotient s/S reflects the retardation in axial diffusion of molecules due to the presence of alveolar walls (Paiva, 1974).

Applications of the solutions of equation (1) incorporate several assumptions:

1. Diffusion is independent of concentration as is the case for molecular diffusion in a binary mixture.
2. Radial diffusion is instantaneous so that there are no radial concentration gradients.

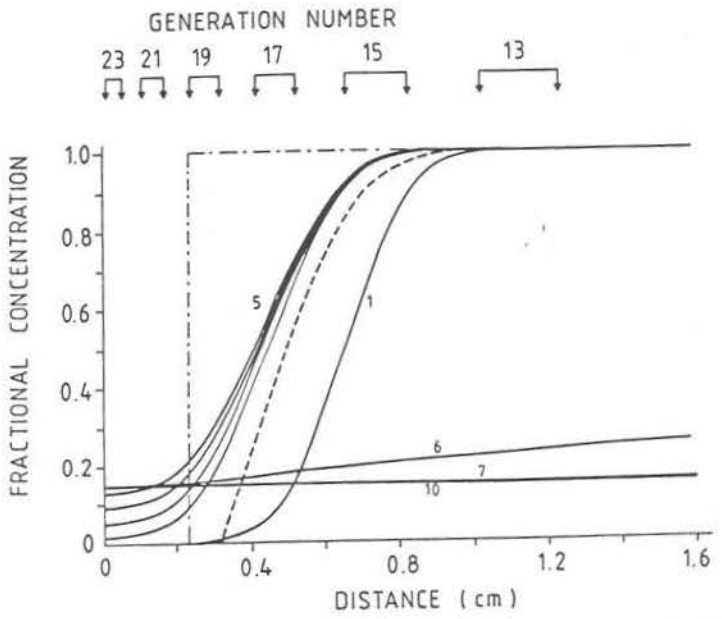

Figure 1 The continuous curves are solutions of equation (1) for a constant flow ($\dot{V}$ = 250 ml/sec) and a 4 sec breath. Inspired gas: oxygen, resident gas: nitrogen. Curves 1 – 10 are the solutions F(x,t) for t = 0.4 n sec with n = 1, ..., 10 (i.e., every 0.4 sec). Curves 1 – 5 correspond to inspiration and 6 – 10 to expiration, curves 5 and 10 being the solutions at end-inspiration and end-expiration, respectively. The vertical dashed-dotted line represents the end-inspiratory concentration profile for D = 0, a condition corresponding to no mixing by molecular diffusion. The dashed curve is the stationary concentration profile computed by Wilson and Lin (1970) in a model also derived from the Weibel data and for an inspiratory O_2 flow of 300 ml/sec. (From Paiva, 1973.)

3. The molecules inside the alveoli do not diffuse axially.
4. The gases are incompressible and the temperature is constant.

These assumptions, in association with the symmetrical Weibel model of the lung, constitute what is usually called the trumpet model.

Figure 1 shows the O_2 concentration profile for an inspiration of 100% O_2 at a constant flow of 250 ml/sec. Curves 1 – 10 are solutions of equation (1) where concentrations 1 and 0 are assumed to be inspired and

residual O_2 concentrations, respectively. Oxygen transfer into blood is neglected. Inspiration and expiration times are equal to 2 sec and the 10 curves are separated by equal time intervals, curves 5 and 10 corresponding to end-inspiration and end-expiration, respectively. It is clear that the O_2–N_2 diffusion front moves into the lung until it becomes quasistationary, despite continuing O_2 flow into the lung. At the level of the alveolar sacs (generation 23 and origin of the model), the convective velocity is zero and the increasing O_2 concentration is due to molecular diffusion alone. During most of the inspiration, the O_2 concentration is constant (100%) in all the generations proximal to generation 15 (for the flow considered). Therefore, the flow by diffusion is zero (according to Fick's law of diffusion) and the transport in this zone is purely convective. Only the last 8 mm of the bronchial tree contains a concentration different from the inspired one. The quantitative contribution of molecular diffusion to O_2 transport can be appreciated by the difference between curve 5 and the dashed-dotted line, which corresponds to the O_2 concentration profile for the same tidal volume of O_2 (500 ml) inspired without diffusion.

A priori, the weakest point of the trumpet model may be thought to be the neglect of convective mixing in the first generations. The existence of the quasistationary front during most of the inspiration shows that whatever the importance of axial spread in the first generations, it can only influence the concentration profile in the zone where the concentration is smaller than 1 (this is not the case for ventilation with very small tidal volumes at a high frequency, where the diffusion front is not established). In this zone the velocities are very small and the molecular diffusion probably approaches total axial mixing.

The solutions of equation (1) represented in Figure 1 also help to explain why the concentrations becomes rapidly constant everywhere in the model (curves 7 – 10) during expiration. Diffusion and convection both contribute to equalize the concentrations. Even in the absence of diffusion, convective movement alone would decrease the concentration gradient of curve 5. However, a small gradient would remain in the last generations. Because of the small distances complete equilibration is achieved by diffusion.

The experiments described in the first part of this section can be understood if we imagine that N_2 is sampled in generation 16 or at a distance of 5 mm from the alveolar end of the model. The dependence of the N_2 concentration on the different parameters of the model becomes clearer if we assume stationary boundary conditions at the model extremes and time-independent (rigid walls) total cross-sections: if during inspiration we assume a constant O_2 concentration of 1 at the model entry and concentration 0 at the alveolar end (justified by the large dilution volume of the

lung with respect to the amount of inspired O_2) a true stationary diffusion front is obtained for O_2. This is represented in Figure 2 for different values of the ratio $\dot{V}/D$. Stationary boundary conditions (100% N_2 at the entry of the model and 20% at the alveolar end) correspond to the experiments by Horsfield et al. (1980) described above.

From Figure 2 it becomes apparent that the front moves peripherally when flow increases, as observed by Fukuchi et al. (1976). Also, if the lung volume decreases, the velocity at a given point increases (inversely proportional to the total cross-section S) and the front moves peripherally. Finally, if we superimpose an oscillatory flow, simulating the to-and-fro cardiogenic flow oscillations, the concentration profile also oscillates. Although the trumpet model provides a good framework for the interpretation of the experimental observations described in this chapter, a major discrepancy with the real lung is the dimension of the airways where the proximal part of the diffusion front is situated: larger than 2.5 mm in real dog lungs and less than 0.7 mm in the model. This difference is probably due to the limitations of the symmetrical geometry, as will be seen in the next section.

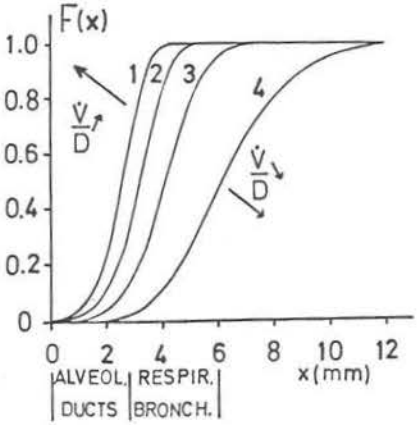

Figure 2 Solutions of equation (1) for steady-state conditions ($\partial C/\partial t = 0$) and time independent geometrical boundaries. The boundary conditions are F = 0 and F = 1 for x = 0 and x = 12 mm, respectively. Curves 1, 2, and 3 correspond to D = 0.1, 0.225, and 0.6 cm^2/sec, respectively, and $\dot{V}$ = 500 ml/sec. Curve 4 corresponds to D = 0.6 cm^2/sec and $\dot{V}$ = 125 ml/sec. (From Paiva, 1985.)

II. Diffusion-Dependent Inhomogeneity of Alveolar Gas

One of the major applications of the concept of the diffusion front is the possibility of dividing the lung into two zones (for a given gas, inspired at a given constant flow). In one, the flow is purely convective and consequently the corresponding branchpoints subtend units that are convection-dependent only. These inhomogeneities are discussed in the next section. The other is the diffusion-dependent zone and the corresponding branchpoints subtend parallel units that are diffusion-dependent. The model analysis suggests that, anatomically, the diffusion-dependent units correspond approximately to the acini (Paiva and Engel, 1984), subtended by terminal bronchioles. If the diffusion front were situated more proximally than suggested by the model analysis, the diffusion-dependent units would be larger and would correspond to groups of acini.

A. Experimental

Multibreath Washouts with Gases of Different Diffusivities

It is well established that for a wide range of experimental conditions, either in excised dog lungs (Okubo and Piiper, 1974) or in human subjects (Lacquet et al., 1975; Kawashiro et al., 1976), the washout of the lighter gas (He or H_2) is always faster than that of the heavier gas (SF_6). Lacquet et al. (1975) computed the Bohr dead space from multibreath washouts and found that the differences between H_2 and SF_6 Bohr dead space increased with increasing flow (at constant frequency). The same authors also found that the mean H_2 concentration is initially greater than that for SF_6. However, after a variable number of breaths a crossover point (COP) occurs following which the relationship is reversed. Von Nieding et al. (1977) studied the COP for end-expired He and SF_6 concentrations and found that in normal subjects breathing with tidal volumes of 700 – 750 ml the COP occurred after four to six breaths. Patients with bronchial asthma in remission demonstrated a COP in the range of that seen in healthy subjects. On the other hand, the COP in patients with severe emphysema was not reached before a mean of 60 breaths.

Closed Circuit Multibreath Wash in with Gases of Different Diffusivities

Using a closed-circuit equilibration with a gas mixture containing He and SF_6, Petrini et al. (1982) have shown that for inspired volumes of 3 liters, the rebreathing dead space of SF_6 exceeded He dead space by more than 200 ml. This is much larger than the Fowler dead space difference between the two gases. Hughes et al. (1982) and Jones et al. (1986) also used a closed circuit He and SF_6 wash in with a 750 ml bag and computed the slope of the logarithm of the difference between mixed expired and equilibration, plotted as a function of breath number (λ) for each gas. Separation of the two gases was quantified by the ratio of the two slopes, $\lambda He/\lambda SF_6$. The major finding was that there was no significant separation between He and SF_6 wash in in supine posture, whereas a significant separation existed in the erect posture, the greatest He – SF_6 separation being observed in the lateral decubitus position. These authors concluded that this effect of position is not compatible with the concept that ascribes a significant portion of the nonuniformity of ventilation in the normal lung to the asymmetrical anatomy of the acinus (see below).

Slope of the Alveolar Plateau

We have shown in Figure 3 the He, SF_6, and N_2 single-breath expirate in a healthy human subject in a seated position, for a 1.1 liter inspiration from a preinspiratory lung volume 0.75 liters above residual volume. The inspired mixture contained 5% He, 5% SF_6, and 90% O_2 and the subject expired to residual volume. The SF_6 slope is larger than that for He, an observation that has always been found in healthy adults. The slopes of He and SF_6 may, however, be similar both in pigs (Kelly et al., 1982a) and in dogs ventilated under special conditions (Meyer et al., 1983). A larger slope for He than for SF_6 has been found in pigs after inhalation of methacholine aerosol (Kelly et al., 1982b).

When the slope of the alveolar plateau was measured simultaneously in the trachea and in small airways larger than 3 mm in diamater, no systematic change was found with airway diameter. The mean slope in the small airways was 77% of that at the trachea (Engel et al., 1974). This indicates that most of the slope is generated within lung zones as small as those subtended by a 3 mm airway. In the dog this corresponds to less than 50 acini.

An important observation was that in normal subjects the slope of the alveolar plateau (performed with a 6.5 sec end-inspiratory breathhold) was little affected by gravity. Indeed, the slope did not differ significantly between maneuvers performed at 0, 1, or 2 g achieved during Lear jet parabolic flights (Michels and West, 1978). This suggests that topographically distributed regional differences do not contribute significantly to the slope measured at the mouth.

With the exception of studies by Meyer et al. (1983), all studies of the slope of the alveolar plateau, starting with those by Fowler (1949), showed a large sensitivity of the slope to breathholding. Engel et al. (1974) showed

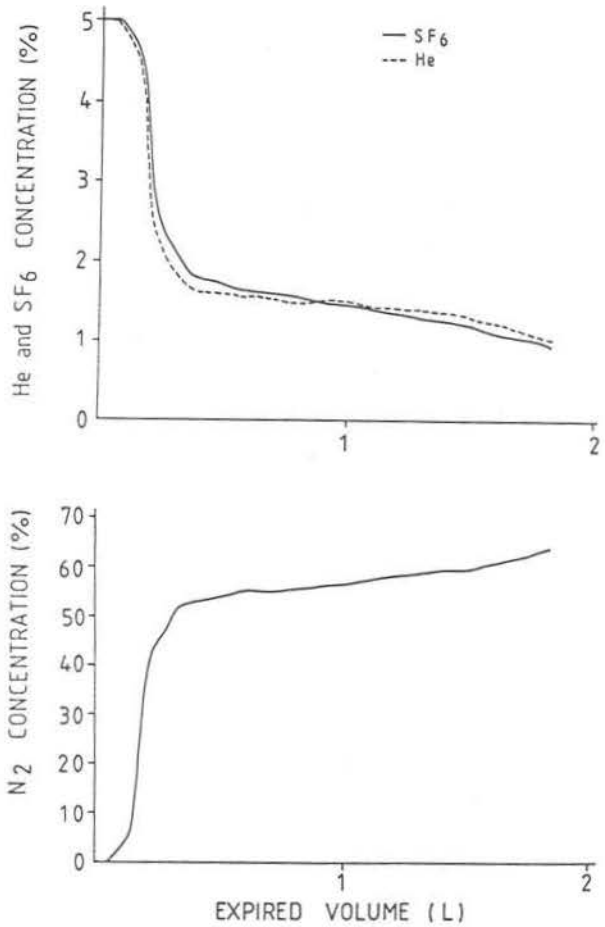

Figure 3 Single-breath washout in a normal subject for a 1.1 liter inspiration from a preinspiratory lung volume 0.75 liter above residual volume. The inspired mixture contained 5% He, 5% SF_6, and 90% O_2 and the subject expired until residual volume.

that the slope, measured in the trachea of anesthetized dogs, changes exponentially with time, falling 7.5% of the initial slope during the first 2 sec of breathholding. Of interest is the fact that simultaneous measurements within a peripheral airway, 3.2 mm in diameter showed a slightly lower initial

slope that decreased by 12.3%/sec during the first 2 sec and by 3.3% of the initial slope per second between 4 and 10 sec of breathholding. The authors suggested that the relatively greater initial rate of decrease reflects the greater diffusion dependence of the slope emanating from small peripheral lung units. In seated normal subjects, a much more rapid decrease of the slope of the alveolar plateau with breathholding has been found, either after 1 liter (Paiva et al., 1984; Crawford et al., 1986b) or an inspiratory capacity inspiration (Paiva et al., 1984). It is apparent from Figure 4 that the normalized slopes (slope divided by the mean-expired N_2 concentration), and consequently the slopes themselves, are almost halved by 4 secs of breathholding.

Hyperbaric Conditions

Although we have not included gas exchange studies in this chapter, it is of interest to mention a puzzling experimental observation: an increased ambient pressure or a higher molecular weight inspired gas mixture paradoxically improves gas exchange as reflected by the $AaDO_2$ (Saltzman et al., 1971; Martin et al., 1972). This has been confirmed by several studies using different methods and experimental conditions.

Van Liew et al. (1979, 1981) studied single-breath washouts using several tracers with different molecular weights at different barometric pressures. Because the molecular diffusion coefficient is inversely proportional to pressure, these experiments offer a direct possibility of measuring the diffusion-dependent inhomogeneity of alveolar gas. The experiments also suggest an independent way of testing the influence of diffusivity since, on the one hand, the inspired mixture contains He and SF_6, the diffusivities of which are in the ratio of 6:1 in air, and, on the other hand, the experiments were performed at pressures of 9.5 and 1.5 Atm, which also corresponds to a ratio close to 6. If the diffusivity were the major determinant of the single-breath expiration profile, one would expect a similar difference between SF_6 and He at 1.5 Atm as between He at 9.5 and 1.5 Atm. Unfortunately, in the experiments reported by Van Liew et al. (1979), the Fowler dead space for He decreased with increasing pressure (their Fig. 2), which suggests a problem with the lag time or response time of the mass spectrometer.

Slope of the Alveolar Plateau during a Multibreath N_2 Washout

The multibreath N_2 washout is usually analyzed by plotting the end-tidal or the mean expired N_2 concentration as a function of breath number or expired volume. In a semilogarithmic plot, the deviation from a straight line is

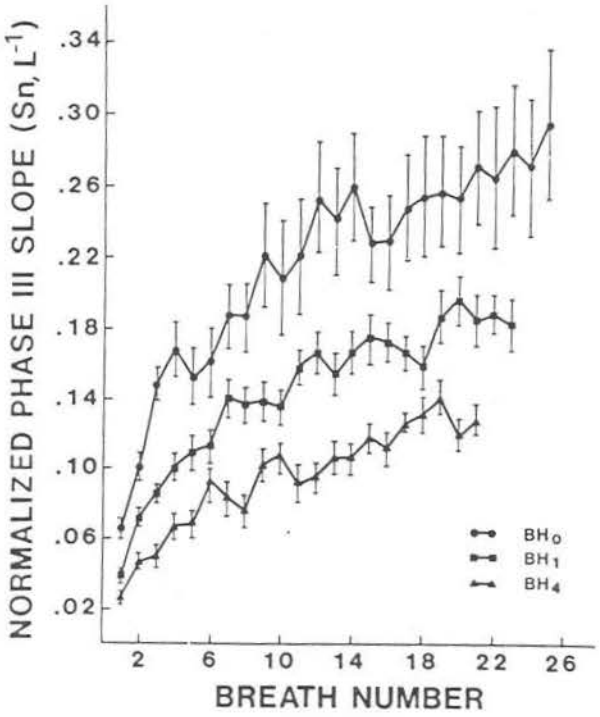

Figure 4 Slope of the alveolar plateau divided by the mean expired N_2 concentration (normalized slope) during a multibreath N_2 washout with a tidal volume of 1 liter and a flow varying between 0.33 and 0.4 liters/sec. BH_0 refers to the control runs; BH_1 and BH_4 correspond to the runs with a 1 sec and 4 sec end-inspiratory breathhold, respectively. The data were obtained from eight runs in five normal subjects and the bars indicate the standard error. (From Crawford et al., 1986b.)

considered an indication of inhomogeneous ventilation. A detailed analysis of the theoretical limits to measurements of uneven ventilation was published by Nye (1961) and addresses the relative insensitivity of the traditional analysis of this test to inhomogeneous ventilation. There are also several practical limitations (Engel, 1985).

If the slope of the alveolar plateau is measured during the whole N_2 washout instead of the first breath only (Fig. 4), several factors contributing to the slope can be identified (Paiva, 1975). Crawford et al. (1985) [illegible] from functional

residual capacity in a seated position, 28% of the slope in a single breath washout was due to inhomogeneities between parallel units subtended by branchpoints proximal to the diffusion front (i.e., in the zone of the lung where the transport is purely convective). Therefore, most of the slope is due to interaction between parallel units subtended by branchpoints situated on the diffusion front and consequently diffusion-dependent. This conclusion was based on the analysis of curves similar to that represented by closed circles in Figure 4. A smooth curve (exponential) was fitted to data points for the breath numbers larger than four, and a partition of the diffusion-dependent and convection-dependent components of the slope could be obtained from the extrapolation of that curve to the origin of the coordinates (Crawford et al., 1985).

In subsequent studies, Crawford et al. (1986a,b) confirmed their previous conclusions. Figure 4 shows not only the rapid decrease of the normalized slope during the first breath with breathholding but also that the rate of increase of the slope after the fourth breath remained unchanged as a function of breathholding time. This indicates that the rate of increase in normalized slope of this part of the curve represents convection-dependent units that behave as predicted by a mathematical model (Paiva, 1975).

B. Theoretical

This section aims to describe models based on physical laws and anatomical data (models of a system) that can provide a theoretical framework for a quantitative explanation of the preceding experimental data. The trumpet model could explain the diffusion-dependent inhomogeneity of alveolar gas based on the different position of the diffusion front for gases of different diffusivities (Paiva et al., 1976). Consequently, the dead space computed from single or multiple breath washouts differed for He (or H_2) and SF_6. Furthermore, there was a good agreement between Bohr dead space measured in multibreath washouts for different frequencies and tidal volumes (Lacquet et al., 1975) and simulations (Paiva et al., 1976) with the trumpet model based on the anatomical data of Hansen and Ampaya (1975). The most interesting aspect of those simulations was that the agreement with experimental results was obtained without the use of any adjustable parameter. However, most of the other experimental observations described in this section could not be explained.

Part of the unresolved problems can be clarified utilizing the concept of interdependence of transport by convection and diffusion in the lung periphery (Paiva and Engel, 1979): this concept may be grasped by considering two identical parallel units with unequal volume expansion and volume flows (Fig. 5). When the branchpoint is positioned proximally to

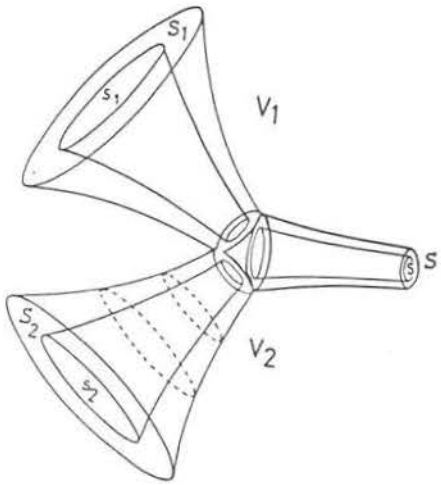

Figure 5 Lung model of two trumpet-shaped units with common stem joining at branchpoint. S, S_1, and S_2 represent total cross-sectional area including alveoli: s, s_1, and s_2 refer to cross-sections of conducting airways only. V_1 refers to the volume of the trumpet with the longer pathway; V_2 is the volume of the trumpet extending from the branchpoint to the dashed line, the position of which is made to vary. (From Paiva and Engel, 1981.)

the diffusion front, gas transport into and out of the two units is purely convective and alveolar concentrations are in proportion to the volume expansions of the units. Diffusion flow, proportional to concentration gradient and cross-section, is zero and there is no diffusive interdependence between the units. In the units subtended by distal branchpoints (at the level of the respiratory bronchioles), diffusive transport becomes significant and helps to equalize parallel concentration differences despite the same inequality of volume flows.

In the periphery of the lung, there is an inequality of volume flows due to acinar asymmetry (Hansen and Ampaya, 1975). This is schematically represented by the dashed lines in Figure 5 that impose $V_2 < V_1$. Homogeneous expansion of the lung results in each unit receiving a flow in proportion to its volume. This by itself would not generate concentration inhomogeneities. However, the diffusive flow in the smaller unit (per unit of volume) is larger than that in the larger unit. Thus, the concentration of inspired gas in the shorter (smaller) unit is greater than in the longer unit. This mechanism may not be obvious intuitively since molecular diffusion is usually regarded as a process leading to equalization of gas concentration. In this case, because diffusion and convection are not independent (but interact through a matter balance constraint) at the branchpoints, an inhomogeneous gas concentration appears, even in a structure expanding homogeneously and isotropically.

The aforementioned mechanism leads to an inhomogeneous N_2 concentration in the parallel units of the lung periphery. This is a necessary but insufficient condition for an N_2 sloping alveolar plateau. However, during expiration, there is also an interdependence of gas transport at the branchpoint (Luijendijk et al., 1980; Paiva and Engel, 1981). Some of the N_2 expired from the larger unit to the branchpoint initially diffuses back into the shorter unit (countercurrent) because of the small convective flow from this unit due to its small volume. During expiration, the concentration differences between the parallel units decrease and consequently progressively more N_2 is available to go out of the model, producing a sloping alveolar plateau. The magnitude of the slope is therefore a consequence of a large number of parameters: structure of the branchpoint region (in the zone of the diffusion front), whose location is itself a consequence of flow; the diffusion coefficient; and the volume of the units subtended by the branchpoint, which determines the convective flows at the branchpoint.

Figure 6 is a quantitative representation of the O_2 concentration profiles in a model where the volume ratio between the parallel units is 0.12. The simulation corresponds to a 1 liter O_2 inspiration at a constant flow of 1 liter/sec. The ordinate is the O_2 concentration and the abscissa (x) is the distance from the terminal end of the longer unit. The dashed and the solid lines are the O_2 concentrations in the shorter and longer units, respectively. The numbers 5 – 10 represent concentrations at 0.2 sec intervals. Curves 5 and 5′ correspond to the end of the inspiration (beginning of the expiration). The inset represents O_2 concentration at the model exit plotted against expired volume. The N_2 concentration profile would be the mirror image of that for O_2, the sum of both concentrations being equal to one. The slope of the alveolar plateau at end-expiration in this example is 7%/liter. This is an unrealistic value due to the large asymmetry chosen to illustrate the phenomenon.

An equivalent description of the interdependence concept can be given by a model with two volumetrically equal parallel units, with a narrowing of one unit at the branchpoint (De Vries et al., 1981; Kelly et al., 1982b). If the branchpoint is in the zone of the diffusion front, the smaller diffusion flow into the narrowed unit, during inspiration, creates a concentration inhomogeneity despite identical volume change in both units. During expiration, countercurrent diffusion of N_2 from the narrowed unit into the nonnarrowed one can also produce a sloping alveolar plateau by the same mechanism as discussed for the single branchpoint asymmetrical model. How does the concept of interdependence help in the interpretation of previously described experimental observations? We will analyze them briefly within the framework of the single branchpoint model.

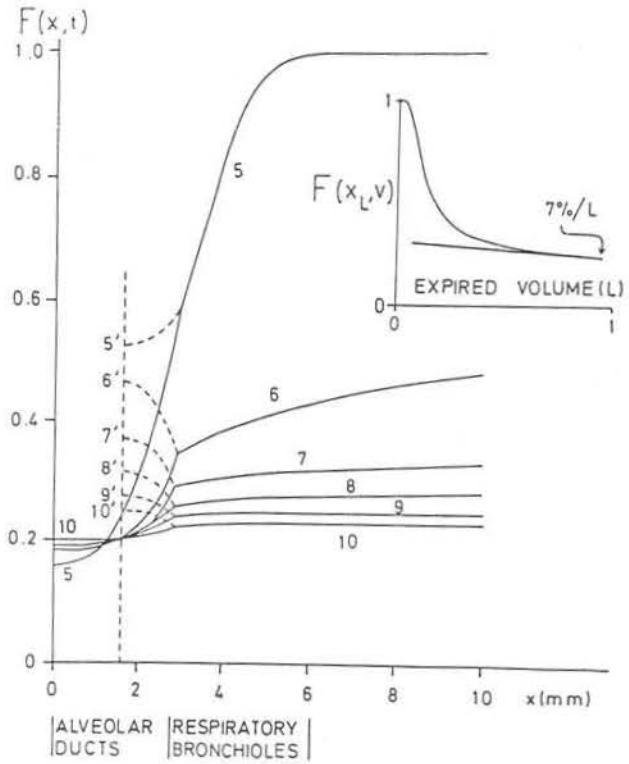

Figure 6 Pattern of O_2 concentration (F) during expiration after 1 liter inspiration of O_2 at 1 liter/sec into an asymmetrical two-trumpet model ($V_2/V_1 = 0.12$). Dashed lines: shorter unit (volume V_2); solid lines: longer unit, (volume V_1), and common pathway. Branchpoint is at x = 2.7 mm. Numbers 5 – 10 represent concentration at 0.2 sec intervals as a function of distance (x) from the terminal surface. Inset: O_2 concentration at exit of model (generation 13/14) plotted against volume expired. (From Paiva and Engel, 1981.)

Multibreath Washouts with Gases of Different Diffusivities

In the multibreath washouts with He and SF_6 performed by Von Nieding et al. (1977), the end-expired concentrations of He and SF_6 were measured. The authors measured the number of breaths to the crossover point in the washouts of the two gases. De Vries et al. (1981) used a single branchpoint model with identical parallel units, but one with a very small cross-section at the branchpoint, to simulate the same experiments. They showed elegantly that a shift in the crossover point was predicted due to the cross-sectional asymmetry of the two parallel units at the branchpoint.

Closed Circuit Multibreath Wash in with Gases of Different Diffusivities

The interpretation of multibreath washouts is complex, and adding one more compartment as a rebreathing bag does not simplify the analysis. The results of Petrini et al. (1982), showing a much greater dead space for SF_6 than for He, may be explained using the trumpet model (Paiva et al., 1976) since the experimental and simulated dead spaces are reasonably close. However, the trumpet model cannot explain why the Bohr dead spaces are much larger than Fowler dead spaces. The single branchpoint model also simulates Bohr dead spaces only slightly greater than Fowler dead spaces. Probably the results of Petrini et al. can only be explained with the incorporation of convection dependent inhomogeneous parallel units (see next section).

The experimental results of Jones et al. (1986) described previously in this section (no separation of He-SF_6 in supine posture) have recently been simulated (Van Muylem et al., 1987). The model used consisted of two diffusion-independent parallel units with two "personal" and one common dead space that differed for He and SF_6. The separation of the two gases (as defined by Jones et al.) was insensitive to the distribution of alveolar volumes but increased significantly when the ratio of tidal volumes to the two units decreased below 0.2. These model simulations suggest that differences between He and SF_6 wash in curves during rebreathing may be generated by large inequalities in convection-dependent ventilation distribution and/or differences in series dead space between the two gases. Hence separation of He-SF_6 wash in curves may not constitute a sensitive index of gas mixing within the lung periphery.

Slope of the Alveolar Plateau

One of the major difficulties in interpreting the slope of the alveolar plateau stems from the many different factors that influence it simultaneously. Furthermore, their relative contribution to the slope varies according to the maneuver performed. At least four factors should be considered.

1. Gas exchange: This factor was extensively studied by Cormier and Bélanger (1983). The final value given by this group to the contribution of gas exchange to the total slope was 10% in healthy subjects in the seated position.

2. Gravity-dependent sequential emptying of units (topographically distributed) with different ΔV/Vo (Milic-Emili et al., 1966; Anthonisen et al., 1970).
3. Gravity-independent diffusion-independent units: These units (intraregional) correspond to those proximal to the diffusion front. They are convection-dependent only. The mechanism corresponding to this factor is probably the intraregional elastic inhomogeneities of the lung (Fukuchi et al., 1980; Crawford et al., 1986a).
4. Gravity-independent diffusion-dependent units: These units are subtended by branchpoints situated on the diffusion front. The mechanism corresponds, at least in part, to the interdependence of transport by convection and diffusion within the acini.

The single branchpoint model with unequal cross-sections of the parallel units at the branchpoint is used to explain the observations (Kelly et al., 1982b) that the He slope may be larger than the SF_6 slope. It was assumed that the proximal airways (where the He front is situated) were affected more by methacholine deposition than those located more peripherally (in the zone of SF_6 diffusion front). The single branchpoint model also facilitated explanation of the slope's dependence on inspiratory and expiratory flows (Lacquet and Van Muylem, 1982).

A major limitation of the single branchpoint model is the fact that it cannot take into account the diffusive interaction among serially distributed branchpoints. This led to the development of the multibranchpoint models (MBPM). Two of them have been compared with experimental data (Bowes et al., 1982, 1985; Paiva and Engel, 1984; Paiva et al., 1984; 1986). Although the qualitative agreement is usually quite good, a feature of these models is that they are exquisitely sensitive to the acinar structure chosen. For example, if we choose arbitrarily an acinar geometry that is very asymmetrical in the proximal part and symmetrical in the periphery, the MBPM will simulate a He slope larger than the SF_6 slope. Unfortunately, the available anatomical data for acinar geometry are still very scanty.

Hyperbaric Conditions

The experiments with inert gases under hyperbaric conditions reported in the literature added little to the understanding of diffusion-dependent mechanisms. Indeed, as clearly explained by Van Liew et al. (1981), the much larger separation between He and SF_6 in hyperbaric conditions can be readily explained on the basis of the peripheral displacement of the distal

position of both diffusion fronts (Paiva et al., 1976), combined with the very large increase in the total cross-section of the airways (trumpet shape) as one moves distally within the acini. However, hyperbaric studies are a valuable approach that may add insights to the field and certainly can add data on values for D that are not accessible in other ways.

Slope of the Alveolar Plateau during a Multibreath N_2 Washout

If the interdependence mechanisms were the only determinant of the slope of the alveolar plateau, the normalized slope during a multibreath N_2 washout would increase during the first four or five breaths (open circles of Fig. 7) and remain constant thereafter (Paiva et al., 1982). It is clear from Figure 4 that this is not the case. We will show in the next section that the explanation of these curves requires the combination of two models based upon different mechanisms. The rapid decrease of the normalized slopes indicates that for 1 liter breaths at functional residual capacity, the ventilation maldistribution occurs mainly in the periphery of the lung (Crawford et al., 1986b). This is in agreement with MBPM simulations, which also

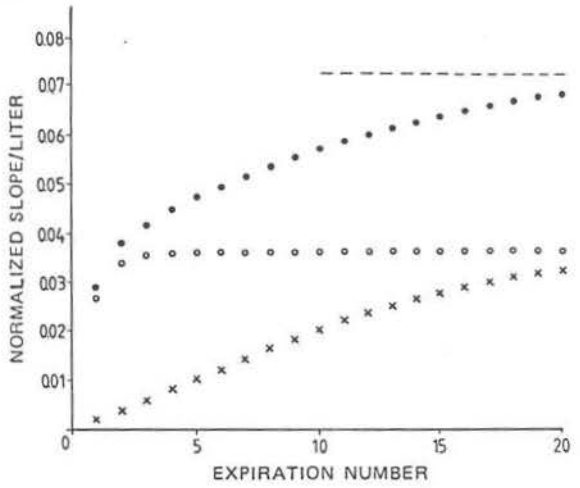

Figure 7 Normalized slope of the alveolar plateau plotted against the expiration number simulated using two models: a two-trumpet model with $V_2/V_1 = 0.39$ (open circles) and a model with two diffusion-independent parallel units with different ventilations and emptying sequences during expiration (crosses). The closed circles are the sum of the normalized slopes simulated by each model.

have shown a rapid homogenization of concentrations during 10 sec of breathholding (Paiva and Engel, 1984).

The mechanism responsible for the rapid stabilization of the diffusion-dependent contribution to the slope during first few breaths can be explained on the basis of simulations using the single-branchpoint model (Paiva et al., 1982): before the first O_2 inspiration, the N_2 concentration is homogeneous in the two parallel units of the model (Fig. 5). During the first inspiration, the difference in concentration between the two units increases and reaches a maximum at a time approximately equal to the end of the inspiration (Fig. 6). During expiration, the concentration difference decreases continuously, producing a slope of the alveolar plateau, but at the end of expiration a concentration difference still persists (curves 10 and 10′ in Fig. 6). This difference then constitutes the initial conditions for the subsequent breath at the end of which the concentration difference between the parallel units (divided by the mean alveolar concentration) is greater. After a few breaths this relative difference of concentration becomes constant and so does the normalized slope.

Although the genesis of the diffusion-dependent part of the slope of the alveolar plateau is not yet completely understood, the models described constitute a basis for its quantitative description.

III. Convection-Dependent Inhomogeneities

A. Experimental

Regional or Topographical Inhomogeneities

We only describe here the most pertinent results since this subject has been recently reviewed (Hughes and Amis, 1985; Milic-Emili, 1986; Engel, 1986). The introduction of radioactive isotopes and particularly ^{133}Xe led to the quantitative study of regional ventilation and the demonstration of topographical inhomogeneities. For example, a small bolus of ^{133}Xe inhaled at functional residual capacity is distributed preferentially to the dependent parts of the lung (Ball et al., 1962). However, the inhomogeneity of regional distribution of gases decreases when inspired flow increases (Robertson et al., 1969). When the preinspiratory lung volume approaches residual volume, airway closure in the dependent lung regions determines the distribution of gas flow, and the inhaled bolus goes preferentially to upper lung regions (Dollfus et al., 1967).

A major step in the understanding of regional ventilation distribution was the demonstration by Milic-Emili et al. (1966) of a static vertical gradient of expansion; the dependent lung regions are less expanded than the nondependent ones at any lung volume, all regions being uniformly expanded at total lung capacity. This is represented schematically in the lower panel of Figure 8. When a full inspiration of O_2 is taken at any preinspiratory lung volume, the N_2 concentration will be always larger in the top of the lung. Therefore, an apicobasal gradient in gas concentration is established. Furthermore, the apical lung regions contribute progressively greater proportions of their initial volume in the course of expiration (Anthonisen et al., 1970) and consequently a positive N_2 slope is generated. All studies have demonstrated a vertical gradient in ventilation, the dependent region receiving approximately twice the ventilation of the apical lung region in upright subjects. Either for a tidal inspiration of O_2 or for an inert gas bolus inhaled at residual volume, the expired N_2 or inert gas concentration profile results in a phase IV following the phase III or alveolar plateau. The height of phase IV is representative of the apex-to-base differences in tracer gas concentration.

Intraregional Inhomogeneities

The term *intraregional* was first associated with the region seen by an external scintillation detector and arose from studies using ^{133}Xe. In most of these there were six detectors on each side of the chest, which corresponds approximately to regions of 0.5 liters at functional residual capacity. The inhomogeneities within such a region are called intraregional and were demonstrated from single-breath washouts measured by intrapulmonary gas sampling. Most of the slope of the alveolar plateau is still present when the sampling site is in airways 3 mm in diameter. Young and Martin (1966) first suggested an intralobar sequence of filling and emptying in humans, based on intralobar sampling. Engel et al. (1974) estimated the dispersal of $\Delta V/Vo$ from cardiogenic oscillations in peripheral airways of open-chest supine dogs. Their results suggested a marked inhomogeneity of ventilation within small subsegments.

Lung volumes at the sublobar level have been measured only recently: Olson and Rodarte (1984) implanted parenchymal markers in isolated dog lobes and measured the deformation of tetrahedrons with volumes ranging from 0.2 to 25.1 ml at total lobar capacity. The authors demonstrated considerable nonuniformity of volume changes. Furthermore, the variability of volume expansions did not follow any topographic orientation and the same behavior was present in both air- and saline-filled lobes. The latter result suggests that surface tension hysteresis is not a major determinant of these inhomogeneities.

B. Theoretical

Regional or Topographic Inhomogeneities

A very useful model that gave a quantitative basis for the interpretation of the inhomogeneity of regional ventilation is the electrical analog of gas

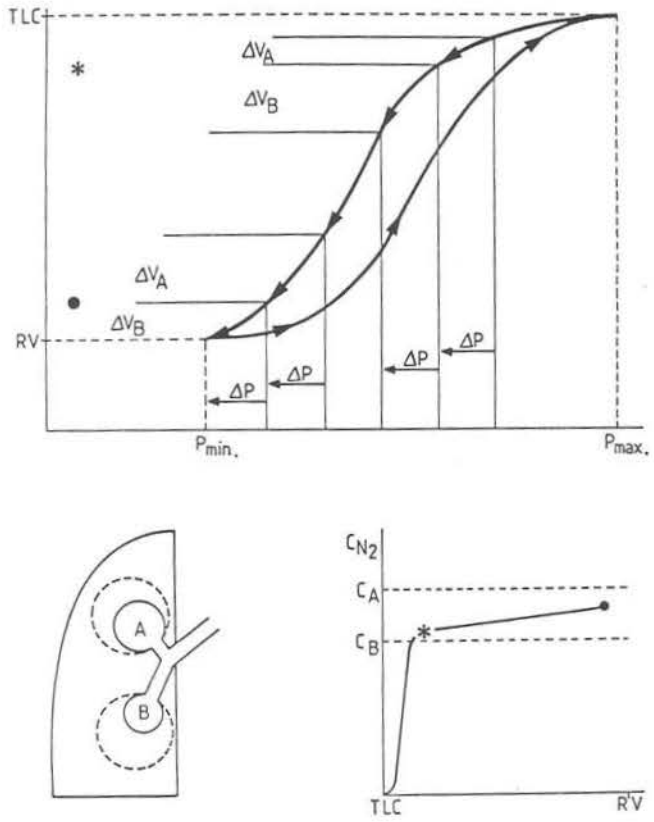

Figure 8 Lower left panel: Schematic representation of upper (A) and lower (B) lung units at residual volume (continuous circles: $V_A > V_B$) and at total lung capacity (dashed circles: $V_A = V_B$). For a vital capacity inspiration of O_2, the N_2 concentration in unit A is higher than in unit B (lower right panel). The pressure-volume loop for a vital capacity breath is represented in the upper panel (downward arrows for the expiratory limb). This diagram aims at explaining schematically that if the vertical gradient of pleural pressure remains constant during expiration (ΔP between unit A and B), unit B contributes more ($\Delta V_B > \Delta V_A$) at the beginning of the expiration (expired concentration represented by a star) and unit A contributes more ($\Delta V_A > \Delta V_B$) at the end (expired concentration represented by a closed circle). This mechanism generates a sloping alveolar plateau (lower right panel).

motion in the lung (Otis et al., 1956). The volume of gas (ΔV) going to a lung unit at a given flow rate $\dot{V}$ is related to the pressure swing (ΔP), the compliance of the unit (C), and the resistance of its airway (R) by the equation

$$\Delta P = \frac{\Delta V}{C} + \dot{V}R \qquad (2)$$

If we consider two parallel units A and B, the nonuniformity of ΔP, C or R may result in convection-dependent inhomogeneities. Let us assume first that ΔP is constant: when $\dot{V}R \ll \Delta V/C$ (or $\dot{V} \ll \Delta V/RC$, where RC is the mechanical time constant), it is apparent from equation (2) that $\Delta V_A/\Delta V_B \approx C_A/C_B$. This means that when convection flow is low, the convection distribution is determined by inequalities in compliance. When flow increases, the resistance becomes nonnegligible and for $\dot{V}R \gg \Delta V/C$ equation (2) predicts that $\dot{V}_A R_A \approx \dot{V}_B R_B$. After integration over the inspired volume (assuming time-independent resistances) $\Delta V_A/\Delta V_B \approx R_B/R_A$. For normal subjects breathing quietly, $\dot{V} \ll \Delta V/RC$ and there is evidence that swings in transpulmonary pressure are equal over different lung regions.

The preceding analysis suggests that during quiet breathing the regional inhomogeneity of ventilation is entirely explained by the static mechanical characteristics of the lung. During single inspirations at higher flows, the more uniform regional distribution of inspired gas can be explained either by different time constants in the lung apex and base or by unequal driving pressures. Although both possibilities exist the latter explanation received support from the observation that the flow dependence of apicobasal gas distribution was greater in the supine than the upright posture (Sybrecht et al., 1976). Because regional expansion and therefore time constants are more uniform in the craniocaudal direction in the supine posture (Bake et al., 1967), the greater flow dependence could not be easily attributed to different time constants. Detailed modeling analyses of topographical ventilation inhomogeneities can be found in recent reviews (Milic-Emili, 1986; Engel, 1986).

The interregional component of the slope of the alveolar plateau can be understood from Figure 8. The inhomogeneous preinspiratory lung volume is represented, at residual volume, in the lower left panel by two units A and B with different volumes. After a full inspiration (dashed circles) of O_2, the N_2 concentration is larger in unit A than in unit B (horizontal dashed lines in the lower right panel). The genesis of the sequential emptying during the subsequent expiration may be explained using a sigmoid shaped P–V curve (upper panel): we consider the expiratory limb

(downward arrows) of this curve and assume a constant pressure gradient ΔP (horizontal arrows) applied to units A and B. The P-V curve represents any part of the lung (i.e., we assume uniform mechanical properties). However, because the pressure applied to unit A is more negative (strictly speaking, more subatmospheric) its compliance is lower at the beginning of expiration. For the same variation of pressure, it is obvious from Figure 8 that the total flow is initially weighted preferentially by unit B where the N_2 concentration (asterisk) is lower. Towards the end of expiration, because of the sigmoid shape of the P–V curve the ratio of relative flows from each unit is reversed and the end-expired concentration (closed circle) approaches that in unit A (see also lower right panel).

Intraregional Inhomogeneities

The analysis of the interregional convection-dependent inhomogeneity, represented in Figure 8, can also be applied to intraregional convection-dependent inhomogeneity. However, a fundamentally different assumption is that mechanical properties are not homogeneous and that each unit within a region has a different P–V curve. Although the pressure swing is considered to be the same for each unit, the curves differ in such a way that the units in which the relative variation of volume is smaller undergo a larger change in specific compliance (compliance per unit of volume) during deflation. Therefore, these units contribute relatively more at the end of expiration. Engel and Macklem (1977) used such a model to describe intraregional convection-dependent inhomogeneities. A formal model analysis has been presented by Fukuchi et al. (1980) and Crawford et al. (1986a) and is supported by the above-mentioned experimental results of Olson and Rodarte (1984).

The presence of intraregional inhomogeneity of elastic properties obviously increases the difficulty in differentiating between the mechanisms responsible for the overall ventilation nonuniformity. Fortunately, the analysis of the slope of the alveolar plateau during a multibreath N_2 washout can shed some light on this problem. Theoretical studies predict (Paiva, 1975) that two convection-dependent (diffusion-independent) units of equal resting volume, in which the less ventilated unit empties relatively more at the end of the expiration, generate a normalized slope of the alveolar plateau (slope divided by the mean expired N_2 concentration) that increases in consecutive breaths of a multibreath N_2 washout (crosses in Fig. 7). The asymptotic value corresponds to the maximal relative difference in concentration between the two units and occurs when the better ventilated unit is empty of N_2. Because the convection-dependent mechanism generating the slope is fundamentally different from that due

to diffusion-convection interaction, it is not surprising that the two-trumpet model described in the previous section generates a very different curve (open circles). For the sake of simplicity we have considered model parameters such that the asymptote reached by the two model simulations is the same (Paiva et al., 1982).

If each region can be represented by these two models, we may expect that the normalized slopes representative of a region correspond to the closed circles (Fig. 7), which are the sum of the slopes generated by each model. Strictly speaking, this is only true if the slopes generated by the two-trumpet model are independent of the flow. Indeed, in the presence of intraregional convection-dependent inhomogeneities, the final part of the washout will be weighted by the less ventilated zones within the region and the diffusion-dependent contribution to the normalized slopes would deviate from the open circles curve. However, this approach constitutes the first attempt to differentiate between the convection-dependent and diffusion-dependent determinants of the slope. A quantification of these two factors is suggested by Figure 7 based on the fact that (1) the diffusion-dependent contribution to the normalized slope is almost independent of the breath number and (2) the convection-dependent part of the normalized slope is well represented by a smooth curve (straight line followed by an exponential). Therefore, a curve can be fitted to the experimental points and extrapolated back to the origin of the coordinates (breath number zero) allowing the separation and quantification of the two components of the slope. A detailed analysis using this approach was reported by Crawford et al. (1985), who estimated the convection-dependent contribution to the slope of the alveolar plateau to be 28%. Subsequent studies by Crawford et al. (1986) confirmed that the major component of ventilation maldistribution results from the interaction of convection and diffusion within small peripheral lung units.

The preceding considerations did not distinguish between the two mechanisms potentially responsible for the convection-dependent component of the slope: interregional (gravity dependent) and intraregional (probably gravity independent). It is hoped that multibreath washout studies planned for future Spacelab flights into microgravity environments may resolve this problem. The reduction of the convection-dependent component of the slope when comparing $g = 0$ to $g = 1$ experiments should correspond to the gravity-dependent convection-dependent inhomogeneities.

In conclusion, we may say that during quiet breathing the interregional distribution of ventilation is determined mainly by the regional compliance. In the periphery of the lung the diffusion–convection interaction is the major determinant of the slope but local static mechanical inhomogeneities probably also play a role.

IV. Concluding Remarks

In 1981, a meeting devoted mainly to the subject of this chapter took place in Brussels. Several questions were posed to the participants and we reiterate four of them to summarize some of the progress made in the field during the last few years (Engel, 1981).

1. Is it possible to achieve a semantic uniformity with respect to the diffusive and convection gas flow occurring in the lung?

Although the answer was and still is obviously yes, confusing terms continue to be used. For example, contrary to the general consensus expressed during that meeting, the word "stratification" is still often used and not always with the same meaning. It is now clear that distinction between series ("stratified") and parallel inhomogeneities in the periphery of the lung is impossible because diffusive and convection transport cannot be considered independent when both convection and diffusion flows are of the same order of magnitude (Paiva and Engel, 1979). "Diffusion-dependent" is an acceptable expression for the concentration inhomogeneities in the periphery of the lung. The zone of the lung where these inhomogeneities exist corresponds roughly to the acinus.

2. Can we quantitate diffusion-dependent inhomogeneity by a single diffusive resistance parameter? If so, can the diffusive-resistance be derived from inert gas washouts?

The complexity of intraacinar gas mixing, described in this chapter, probably leads to a negative answer to the first part of the question. However, it may be possible, using a multibreath N_2 washout, to separate convection-dependent from diffusion-dependent inhomogeneity.

3. Can intraacinar asymmetry account completely for the diffusion-dependent inhomogeneity and impairment of gas mixing observed at the mouth?

There is still no answer to this question. Besides the uncertainties regarding acinar anatomy, very little is known about acinar movement. The assumption of homogeneous acinar movement is only the simplest one, hiding our ignorance on the subject. The recent work by Mercer and Crapo (1985) supports the views of Forrest (1970) that the acinus does not move homogeneously. The incorporation of quantitative data of acinar dimensions as a function of lung volume into the multibranchpoint models will be the first step towards answering this question.

4. Do intralobar lung units differ in static mechanical properties? If so, is this difference responsible for the measured impairment of gas mixing and does it contribute to the slope of the alveolar plateau?

The recent experimental work by Olson and Rodarte (1984) gives a positive answer to the first part of this question. However, although intralobar mechanical inhomogeneities probably impair gas mixing, it has not yet been shown that they contribute to the slope of the alveolar plateau.

A major development in the understanding of gas mixing and distribution in the lung periphery during the past decade was the identification of the different factors that may influence the inhomogeneity of ventilation. The next development will be the elaboration of tests enabling the differentiation and quantification of the contribution of each one. A first step was achieved recently by the distinction between convection-dependent and diffusion-dependent inhomogeneities from the multibreath N_2 washout.

References

Anthonisen, N. R., Robertson, P. C., and Roos, W. R. D. (1970). Gravity-dependent sequential emptying of lung regions. *J. Appl. Physiol.*, 28:589–595.

Bake, B., Bjure, J., Grimby, G., Milic-Emili, J., and Nilsson N. Y. (1967). Regional distribution of inspired gas in supine man. *Scand. J. Respir. Dis.*, 48:189–196.

Ball, W. C., Jr., Stewart, P. B., Newsham, L. G. S., and Bates, D. V. (1962). Regional pulmonary function study with $Xenon^{133}$. *J. Clin. Invest.*, 41:519–531.

Bowes, C., Cumming, G., Horsfield, K., Loughhead, J., and Preston, S. (1982). Gas mixing in a model of the pulmonary acinus with asymmetrical alveolar ducts. *J. Appl. Physiol.*, 52:624–633.

Bowes, C., Richardson, J. D., Cumming, G., and Horsfield, K. (1985). Effect of breathing pattern on gas mixing in a model with asymmetrical alveolar ducts. *J. Appl. Physiol.*, 58:18–26.

Cormier, Y., and Bélanger, J. (1983). Quantification of the effect of gas exchange on the slope of phase III. *Bull. Eur. Physiopathol. Respir.*, 19:13–16.

Crawford, A. B. H., Makowska, M., Paiva, M., and Engel, L. A. (1985). Convection-and diffusion-dependent ventilation maldistribution in normal subjects. *J. Appl. Physiol.*, 59:838–846.

Crawford, A. B. H., Makowska, M., and Engel, L. A. (1986a). Effect of tidal volume on ventilation maldistribution. *Respir. Physiol.*, 66:11–25.

Crawford, A. B. H., Makowska, M., Kelly, S., and Engel, L. A. (1986b). Effect of breathholding on ventilation maldistribution in normal subjects. *J. Appl. Physiol.*, 61:2108–2115.

Cumming, G., Horsfield, K., and Preston, S. B. (1971). Diffusion equilibrium in the lungs examined by nodal analysis. *Respir. Physiol.*, 12:329–345.

De Vries, W. R., Luijendijk, S. C. M., and Zwart, A. (1981). Helium and sulfur hexafluoride washout in asymmetric lung models. *J. Appl. Physiol.*, 51:1122–1130.

Dollfuss, R. E., Milic-Emili, J., and Bates, D. V. (1967). Regional ventilation of lung, studied with boluses of ^{133}Xenon. *Respir. Physiol.*, 2:234–246.

Engel, L. A. (1981). Intraregional ventilation distribution. *Bull. Eur. Physiopathol. Respir.*, 18:181–188.

Engel, L. A. (1983). Gas mixing within the acinus of the lung. *J. Appl. Physiol.*, 54:609–618.

Engel, L. A. (1985). Intraregional gas mixing and distribution. In *Gas Mixing and Distribution in the Lung*. Edited by L. A. Engel and M. Paiva. New York, Marcel Dekker, pp. 287–358.

Engel, L. A. (1986). The dynamic distribution of gas flow. In *Handbook of Physiology, Sec. 3: The Respiratory System*, Vol III: Mechanics of Breathing. Edited by J. Mead and P. T. Macklem. Bethesda, MD, American Physiological Society, pp. 575–593.

Engel, L. A., and Macklem, P. T. (1977). Gas mixing and distribution in the lung. *International Review of Physiology*, Vol 14: *Respiratory Physiology* II. Edited by J. G. Widdicombe. Baltimore, University Park Press, pp. 37–82.

Engel, L. A., Menkes, H., Wood, L. D. H., Utz, G., Joubert, J. and Macklem, P. T. (1973a). Gas mixing during breathholding studied by intrapulmonary gas sampling. *J. Appl. Physiol.*, 35:9–17.

Engel, L. A., Wood, L. D. H., Utz, G., and Macklem, P. T. (1973b). Gas mixing during inspiration. *J. Appl. Physiol.*, 35:18–24.

Engel, L. A., Utz, G., Wood, L. D. H., and Macklem, P. T. (1974). Ventilation distribution in anatomical lung units. *J. Appl. Physiol.*, 37:194–200.

Forrest, J. B. (1970). The effect of changes in lung volume on the size and shape of alveoli. *J. Physiol.*, 210:533–547.

Fowler, W. S. (1949). Lung function studies: III. Uneven pulmonary ventilation in normal subjects and in patients with pulmonary disease. *J. Appl. Physiol.*, 2:283–299.

Fukuchi, Y., Roussos, C. S., Macklem, P. T., and Engel, L. A. (1976). Convection, diffusion and cardiogenic mixing: an experimental approach. *Respir. Physiol.*, 26:77–90.

Fukuchi, Y., Cosio, M., Murphy, B., and Engel, L. A. (1980). Intraregional basis for sequential filling and emptying of the lung. *Respir. Physiol.*, 41:253–266.

Hansen, J. E., and Ampaya, E. P. (1975). Human air space shapes, sizes, areas and volumes. *J. Appl. Physiol.*, 38:990–995.

Horsfield, K., Davies, A., Mills, C., and Cumming, G. (1980). Effect of flow oscillations on the stationary concentration front in a hollow cast of the airways. *Lung*, 157:103–111.

Horsfield, K., Gabe, I., Mills, C., Buckman, M., and Cumming, G. (1982). Effect of heart rate and stroke volume on gas mixing in dog lung. *J. Appl. Physiol.*, 53:1603–1607.

Hughes, J. M. B., and Amis, T. C. (1985). Regional ventilation distribution. In *Gas Mixing and Distribution in the Lung*. Edited by L. A. Engel and M. Paiva. New York, Marcel Dekker, pp. 117–220.

Hughes, J. M. B., Jones, H. A., and Davies, E. E. (1982). Applications of multi-breath washin measurements in closed circuit using a mass spectrometer. *Bull. Eur. Physiopathol. Respir.*, 18:309–317.

Jones, H. A., Chakrabarti, M. K., Davies, E. E., Hughes, J. M. B., and Sykes, M. K. (1982). The contribution of heart beat to gas mixing in the lungs of dogs. *Respir. Physiol.*, 50:177–185.

Jones, H. A., Davies, E. E., and Hughes., J. M. B. (1986). A rapid rebreathing method for measurement of pulmonary gas volume in humans. *J. Appl. Physiol.*, 60:311–316.

Kawashiro, T., Sikand, R. S., Adaro, F., Takahashi, H., and Piiper, J. (1976). Study of intrapulmonary gas mixing in man by simultaneous washout of helium and sulfur hexafluoride. *Respir. Physiol.*, 28:261–275.

Kelly, S., Cohen, C., Powell, E., Paiva, M. and Engel, L. A. (1982a). Gas mixing in the lungs of dogs and pigs. *Respir. Physiol.*, 47:341–349.

Kelly, S., Paiva, M. and Engel, L. A. (1982b). Bronchoconstriction and gas mixing in canine and pig lungs. *Bull. Eur. Physiopathol. Respir.*, 18:229–237.

Lacquet, L. M., and Van Muylem, A. (1982). He and SF_6 single-breath expiration curves. Comparison with the Paiva-Engel model. *Bull. Eur. Physiopathol. Respir.*, 18:239–246.

Lacquet, L., Van der Linden, L. P., and Paiva, M. (1975). Transport of H_2 and SF_6 in the lungs. *Respir. Physiol.*, 25:157–173.

Luijendijk, S. C. M., Zwart, A., De Vries, W. R., and Salet, W. M. (1980). The sloping alveolar plateau at synchronous ventilation. *Pflugers Arch.*, 384:267–277.

Martin, R. R., Zutter, M., and Anthonisen, N. R. (1972). Pulmonary gas exchange in dogs breathing SF_6 at 4Atm. *J. Appl. Physiol.*, 33:86–92.

Mercer, R. R., and Crapo, J. D. (1985). Alveolar pressure-volume relationships determined from 3-D reconstruction of alveoli in the rat lung. *Am. Rev. Respir. Dis.*, 131:A325.

Meyer, M., Hook, C., Rieke, H., and Piiper, J. (1983). Gas mixing in dog lungs studied by single breath washout of He and SF_6. *J. Appl. Physiol.*, 55:1795–1802.

Michels, D. B., and West, J. B. (1978). Distribution of pulmonary ventilation and perfusion during short periods of weightlessness. *J. Appl. Physiol.*, 45:987–998.

Milic-Emili, J. (1986). Static distribution of lung volumes. In *Handbook of Physiology*, Sec 3: *The Respiratory System*, Vol III: Mechanics of Breathing. Edited by J. Mead and P. T. Macklem. Bethesda, MD, American Physiological Society, pp. 575–593.

Milic-Emili, J., Henderson, J. A. M., Dolovich, B. M., Trop, D., and Kaneko, K. (1966). Regional distribution of inspired gas in the lung. *J. Appl. Physiol.*, 21:749–759.

Nye, R. E. (1961). Theoretical limits to measurement of uneven ventilation. *J. Appl. Physiol.*, 16:1115–1123.

Okubo, T., and Piiper, J. (1974). Intrapulmonary gas mixing in excised dog lung lobes studie by simultaneous wash-out of two inert gases. *Respir. Physiol.*, 21:223–239.

Olson, L. E., and Rodarte, J. R. (1984). Regional differences in expansion in excised dog lung lobes. *J. Appl. Physiol.*, 57:1710–1714.

Otis, A. B., McKerrow, C. B., Bartlett R. A., Mead, J., McIlroy, M. B., Selverstone, N. J. and Radford, E. P., Jr. (1956). Mechanical factors in distribution of pulmonary ventilation. *J. Appl. Physiol.*, 8:427–443.

Paiva, M. (1972). Computations of the boundary conditions for diffusion in the human lung. *Comput. Biomed. Res.*, 5:585–595.

Paiva, M. (1973). Gas transport in the human lung. *J. Appl. Physiol.*, 35:401–410.

Paiva, M. (1974). Gaseous diffusion in an alveolar duct simulated by a digital computer. *Comput. Biomed. Res.*, 7:533–543.

Paiva, M. (1975). Two new pulmonary functional indexes suggested by a simple mathematical model. *Respiration*, 32:389–403.

Paiva, M. (1985). Theoretical studies of gas mixing in the lung. In *Gas Mixing and Distribution in the Lung*. Edited by L. A. Engel and M. Paiva. New York, Marcel Dekker, pp. 221–285.

Paiva, M. and Engel, L. A. (1979). Pulmonary interdependence of gas transport. *J. Appl. Physiol.*, 47:296–305.

Paiva, M. and Engel, L. A. (1981). The anatomical basis for the sloping N_2 plateau. *Respir. Physiol.*, 44:325–337.

Paiva, M., and Engel, L. A. (1984). Model analysis of gas distribution within human lung acinus. *J. Appl. Physiol.*, 56:418–425.

Paiva, M., and Engel, L. A. (1987). Theoretical studies of gas mixing and ventilation distribution in the lung. *Physiol. Rev.*, 67:750–796.

Paiva, M., Lacquet, L. M., and Van der Linden, L. P. (1976). Gas transport in a model derived from Hansen-Ampaya anatomical data of the human lung. *J. Appl. Physiol.*, 41:115–119.

Paiva, M., Van Muylem, A., and Engel, L. A. (1982). The slope of phase III in multibreath N_2 washout and washin. *Bull. Eur. Physiopathol. Respir.*, 18:273–280.

Paiva, M., Van Muylem, A., Ravez, P., and Yernault, J. C. (1984). Inspired volume dependence of the slope of the alveolar plateau. *Respir. Physiol.*, 56:309–325.

Paiva, M., Van Muylem, A., Ravez, P., and Yernault, J. C., (1986). Preinspiratory lung volume dependence of the slope of the alveolar plateau. *Respir. Physiol.*, 63:327–338.

Petrini, M. F., Peterson, B. T., Hyde, R. W., Lam, V., Utel, M. J., and Kallay, M. C. (1982). Uneven gas mixing during rebreathing assessed by simultaneously measuring dead space. *J. Appl. Physiol.*, 53:930–939.

Piiper, J., and Scheid, P. (1987). Diffusion and convection in intrapulmonary gas mixing. In *Handbook of Physiology*, Sec. 3: *The Respiratory System*, Vol. IV: Gas Exchange. Edited by L. E. Farhi and S. M. Tenney. Bethesda, MD, American Physiological Society, pp. 51–129.

Robertson, P. C., Anthonisen, N. R., and Ross, D. (1969). Effect of inspiratory flow rate on regional distribution of inspired gas. *J. Appl. Physiol.*, 26:438–443.

Saltzman, H. A., Salzano, J. V., Blenkarn, G. O., and Kylstra, J. A. (1971). Effects of pressure on ventilation and gas exchange in man. *J. Appl. Physiol.*, 30:443–449.

Scherer, P. W., Shendalman, L. H., and Greene, N. M. (1972). Simultaneous diffusion and convection in single breath lung washout. *Bull. Math. Biophys.*, 34:393–412.

Sybrecht, G., Landau, L., Murphy, B. G., Engel, L. A., Martin, R. R., Macklem P. T. (1976). Influence of posture on flow dependence of distribution on inhaled ^{133}Xe boli. *J. Appl. Physiol.*, 41:489–496.

Van Liew, H. D., Thalmann, E. D., and Sponholtz, D. K. (1979). Diffusion-dependence of pulmonary gas mixing at 5.5 and 9.5 ATA. *Undersea Biomed. Res.*, 6:251–258.

Van Liew, H. D., Thalmann, E. D., and Sponholtz, D. K. (1981). Hindrance to diffusive gas mixing in the lung in hyperbaric environments. *J. Appl. Physiol.*, 51:243–247.

Van Muylem, A., Engel, L. A. and Paiva, M. (1987). Differences between He and SF_6 washin rates during closed circuit rebreathing; a model analysis. *Bull. Eur. Physiopathol. Respir.*, 23:401s.

Von Nieding, G., Lollgen, H., Smidt, U., and Linde, H. (1977). Simultaneous washout of helium and sulfur hexafluoride in healthy subjects and patients with chronic bronchitis, bronchial asthma, and emphysema. *Am. Rev. Respir. Dis.*, 116:649–659.

Weibel, E. R. (1963). *Morphometry of the Human Lung*. Heidelberg, Springer-Verlag.

Wilson, T. A., and Lin, K. (1970). Convection and diffusion in the airways and the design of the bronchial tree. In *Airway Dynamics Physiology and Pharmacology*. Edited by A. Bouhuys. Springfield, IL, Charles C Thomas, pp. 5–19.

Young, A. C., and Martin, C. J. (1966). The sequence of lobar emptying in man. *Respir. Physiol.*, 1:372–381.

7

Absorption of Soluble Gases and Vapors in the Respiratory System

LINDA M. HANNA and ROBERT FRANK

The Johns Hopkins University
School of Hygiene and Public Health
Baltimore, Maryland

PETER W. SCHERER

University of Pennsylvania
Philadelphia, Pennsylvania

I. Introduction

The respiratory system is an absorptive and excretory surface for inhaled agents, many of which may impair the biochemical, functional, or structural integrity of the respiratory system itself or that of more distant tissues. These inhalants can be diverse, ranging from air pollutants to anesthetics, bacteria, viruses, and allergens. The biologic response induced by these inhaled agents depends on the mechanism of interaction with the target tissue while the magnitude of that response is influenced by the availability of the inhaled agent. Appropriate quantification of this dose is one of the major obstacles to a reliable evaluation of the biologic effects attributable to airborne substances.

Currently, minute ventilation, contaminant concentration, and exposure duration are recognized as parameters affecting the biologic response (Adams et al., 1981; EPA, 1986). More fundamentally, however, these parameters exert their influence by affecting the transport of the agent within the respiratory system and, hence, the airway region in which the agent is principally absorbed or deposited. The principal absorption site can be an important determinant of the effect and fate of an inhaled agent. This